

# The Scattering and Neutrino Detector at the Large Hadron Collider in CERN

Natalia Polukhina <sup>1,2,\*</sup>, Nina Konovalova <sup>1,2</sup> and Tatiana Shchedrina <sup>1,2</sup> <sup>1</sup> Lebedev Physical Institute, Russian Academy of Sciences, Moscow 119991, Russia<sup>2</sup> Megascience Center, National University of Science and Technology MISiS, Moscow 119049, Russia

\* Correspondence: natalia.polukhina@cern.ch

**Abstract:** SND@LHC (Scattering Neutrino Detector at the Large Hadron Collider) is a compact and stand-alone experiment to perform measurements with neutrinos produced in the LHC in a hitherto unexplored pseudorapidity region of  $7.2 < \eta < 8.6$ . The experiment is located in the T118 (Target line 18) LHC tunnel, 480 m downstream of the ATLAS detector interaction point. The SND@LHC detector is composed of a hybrid system based on an 800 kg target mass of tungsten plates, interleaved with emulsion and electronic trackers, followed downstream by a muon system. This configuration allows us to distinguish all three neutrino flavors, opening a unique opportunity to probe the physics of heavy flavor production in the LHC in a region that is not accessible to the ATLAS, CMS, LHCb and FASER experiments. The detector concept is also well suited to searching for feebly interacting particles via signatures of scattering in the detector target. The first phase of the experiment has been carried out during the ongoing LHC Run 3, and the first data of the LHC Run3 commissioning period are being processed and analyzed.

**Keywords:** new LHC experiment; emulsion neutrino target; neutrino interactions; identification of neutrino flavors



**Citation:** Polukhina, N.; Konovalova, N.; Shchedrina, T. The Scattering and Neutrino Detector at the Large Hadron Collider in CERN. *Physics* **2023**, *5*, 499–507. <https://doi.org/10.3390/physics5020035>

Received: 22 February 2023

Revised: 23 March 2023

Accepted: 29 March 2023

Published: 20 April 2023



**Copyright:** © 2023 by the authors. Licensee MDPI, Basel, Switzerland. This article is an open access article distributed under the terms and conditions of the Creative Commons Attribution (CC BY) license (<https://creativecommons.org/licenses/by/4.0/>).

## 1. Introduction

The Large Hadron Collider (LHC), today's highest-energy proton-proton ( $pp$ ) collider, is a unique facility for the study of neutrinos in an energy range (from 350 GeV to several TeV) which has been inaccessible so far. The high intensity of  $pp$  collisions achieved by the LHC machine produces a large neutrino flux in the forward direction, and the high neutrino energies imply relatively large neutrino–nucleon cross-sections. Neutrinos in  $pp$  interactions in the LHC arise from leptonic W and Z boson decays (the pseudorapidity region,  $4 < \eta < 5$ , as well as  $b$  and  $c$  quark decays ( $\eta > 7$ )).

The Scattering Neutrino Detector experiment at the LHC—SND@LHC experiment [1–3]—to study high-energy neutrinos at the LHC was approved by CERN (the European Organization for Nuclear Research in Geneva, Switzerland) on March 2021, and the detector installation was completed in December 2021. The detector is located slightly off the  $pp$  beam axis, although very close to it. An intense and highly collimated (within polar angles of less than 2.5 mrad) beam of the produced neutrinos passes through the detector. The pseudorapidity region under study ( $7.2 < \eta < 8.6$ ) is complementary to all of the other experiments in the LHC, including the similar experiment FASER [4].

The off-axis detector arrangement is ideal for studying the production of heavy quarks in the unexplored pseudorapidity range. Unlike  $\nu_\tau$  and  $\bar{\nu}_\tau$  originating exclusively from heavy hadron decays,  $\nu_e$  and  $\bar{\nu}_e$  mainly come from charmed hadron decays with a small admixture from kaons at low energies, where the interaction cross-section in the detector is lower, while  $\nu_\mu$  and  $\bar{\nu}_\mu$  show significant contribution from pion and kaon decays. In the proposed pseudorapidity range,  $\nu_\mu$  from  $\pi$  and  $K$  decays show a softer energy spectrum. This allows us to distinguish between components from charm and from  $\pi/K$  decays by measuring neutrino energy. Since in this range of pseudorapidity, a large fraction of the

neutrinos originate from charmed-hadron decays, the neutrinos can be seen as being a probe of heavy-flavor production. Moreover, the SND@LHC experiment is sensitive to feebly interacting particles (FIPs) [5] via the FIPs' scattering-off atoms in the detector target [6]. The new particles scatter similarly to neutrinos, such as light dark matter (LDM) particles that interact with the standard model particles via portal mediators, playing the role of FIPs. The direct search strategy gives the experiment sensitivity in a region of the FIP mass-coupling parameter space that is complementary to other indirect searches. In detail, the physics goals of the SND@LHC experiment are set forth in the technical proposal [1].

Given the expected LHC integrated luminosity during 2022–2025 ( $290 \text{ fb}^{-1}$ ), about two thousand high-energy neutrino interactions is expected to be observed and studied by SND@LHC. The neutrino flavor can be identified in charged-current (CC) interactions via the identification of the corresponding charged lepton produced in the final state. The expected energy spectrum of incoming neutrinos and anti-neutrinos in the pseudorapidity range covered by the SND@LHC detector normalized to the integrated luminosity is presented in Figure 1 [3], which illustrates the leading contribution of muon neutrinos (73%) and electron neutrinos (25%).

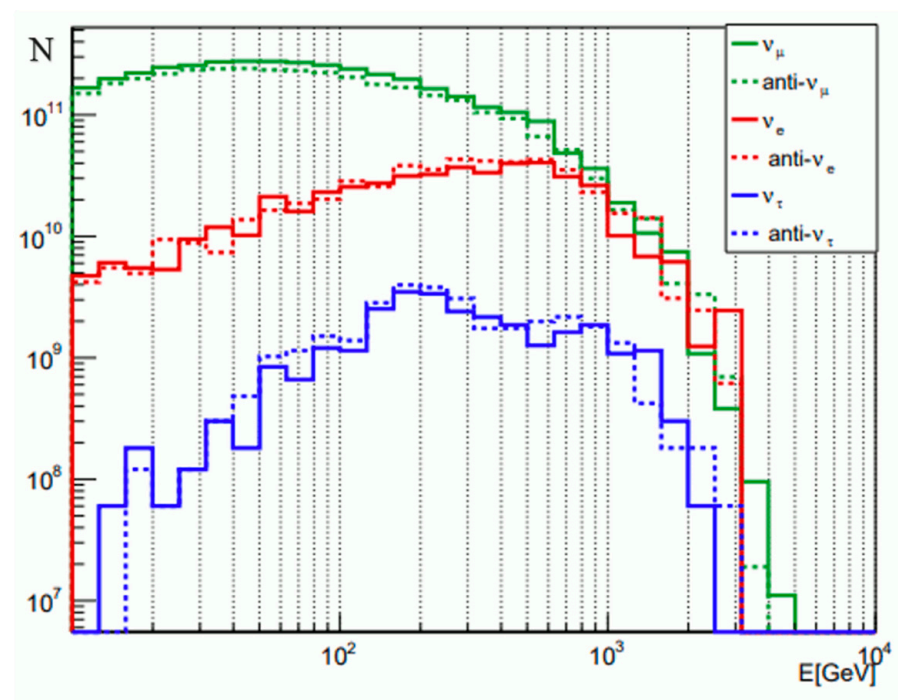


**Figure 1.** Energy spectrum of the different types of incoming neutrinos and anti-neutrinos as predicted by the DPMJET/FLUKA [7,8] simulation. The result of the simulation has been normalized to produce neutrino spectra for  $290 \text{ fb}^{-1}$  [3].

## 2. Detector

The detector (Figure 2) was designed to find the best compromise between geometrical constraints and the following physics requirements: a good calorimetric measurement of the energy requiring about  $10 \lambda_{\text{int}}$  (where  $\lambda_{\text{int}}$  is the interaction mean free path), a good muon identification efficiency requiring enough material to absorb hadrons and a transverse size of the target region having the desired azimuthal angular acceptance.

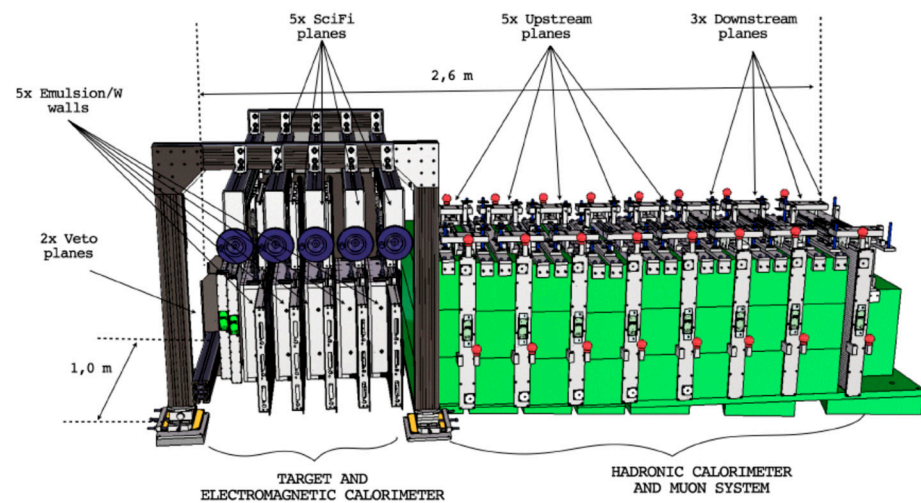


**Figure 2.** The SND@LHC detector concept. See text for details.

The Upstream Veto Detector (UVD) located upstream of the target acts as a veto for charged particles, mostly muons coming from the ATLAS detector interaction point. The baseline technology for the UVD is scintillating bars readout by silicon photomultipliers (SiPMs) that tag incoming muons.

The neutrino target, designed according to the Emulsion Cloud Chamber (ECC) technology [9], acts as a vertex detector. The ECC technology makes use of nuclear emulsion films interleaved with passive layers to build up a tracking device with a sub-micrometric position and milliradian angular resolution, as in the OPERA experiment [10,11]. It is capable of detecting  $\tau$  leptons and charmed hadrons by disentangling their production and decay vertices [12]. It is also suitable for FIP detection through the direct observation of their scattering-off electrons or nucleons in the passive plates. The high spatial resolution of nuclear emulsion films allows for identifying electrons by observing electromagnetic showers in the brick.

The SND@LHC neutrino target and vertex detector is made of five walls with a sensitive transverse size of  $384 \times 384 \text{ mm}^2$ , and it amounts to 830 kg. Each wall consists of four cells (bricks), made of 60 emulsion films, interleaved with 1 mm tungsten plates. Tungsten was selected as the target material in order to maximize the interaction rate per unit volume. Its small radiation length allows for good performance in the electromagnetic shower reconstruction. The resulting brick has a mass of 41.5 kg and a total thickness of  $\sim 78 \text{ mm}$ , making  $\sim 17 X_0$ , where  $X_0$  is the radiation length. A schematic of one wall is shown in Figure 3. The entire SND@LHC neutrino target contains 1200 emulsion films, for a total of about  $44 \text{ m}^2$ .

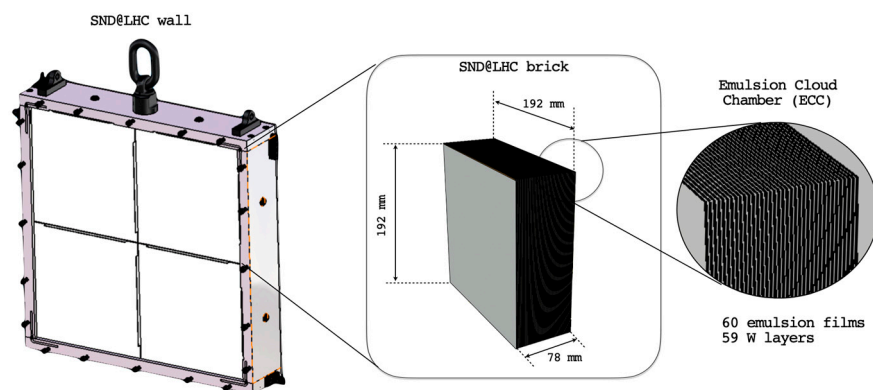
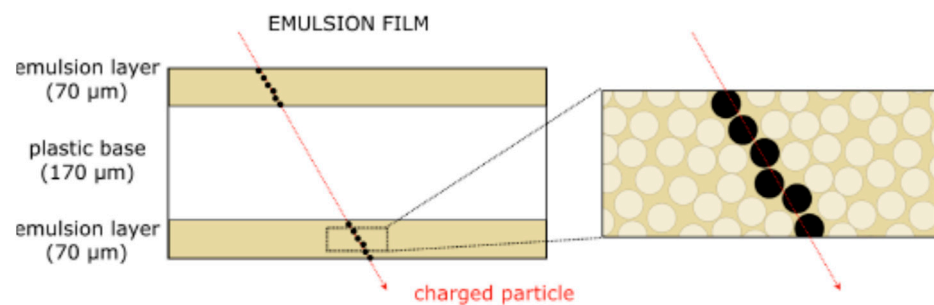


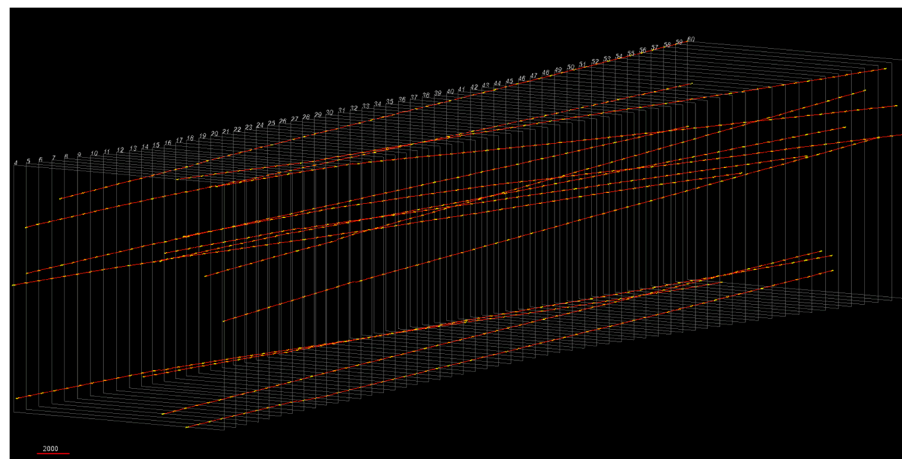
**Figure 3.** A schematic of one wall of the target SND@LHC neutrino target and vertex detector.

Each of the five walls of the ECC is followed by a scintillating fiber (SciFi) plane. The use of the SciFi detectors makes it possible to measure the position of the neutrino interaction in the emulsion block and complements the emulsion target, amounting to a total of 85 X0, for the calorimetric measurement of electromagnetic showers. SciFi also connects the reconstructed emulsion track with the muon candidate track identified by the muon detector.

A nuclear-emulsion plate consists of two sensitive emulsion layers, each poured onto a plastic substrate. The reconstruction of the so-called micro-tracks, which are the tracks traversing each sensitive layer of an emulsion plate, is performed in the process of online scanning. The  $xy$  coordinate plane is related to the surface of the emulsion plate. Since an emulsion film is formed by two emulsion layers, the connection of the two micro-tracks through the plastic base provides a reconstruction of the particle's trajectory in the emulsion film, called a base-track. The reconstruction of particle tracks in the full volume requires connecting the base-tracks in consecutive films (Figure 4a). The track reconstruction in the emulsion target is performed using a Kalman filter seeded on the base-tracks recorded in the single emulsion films. An example of the track reconstruction is presented in Figure 4b. Comparing the position and angle of each base-track with a linear fit on the  $xz$  and  $yz$  planes leads to an estimation of the tracking resolution. The  $z$  axis is directed along the beam.



(a)



(b)

**Figure 4.** (a) The charged particle track in an emulsion film. (b) The tracks reconstructed in the emulsion target; randomly selected 15 tracks in 57 emulsion layers in a  $1 \times 1 \text{ cm}^2$  area (Emulsion Run 0 data).

The muon detector is located downstream of the ECC/SciFi target detector. It identifies muons, crucial to identifying the muon neutrino CC interactions. The muon identification system consists of iron slabs interleaved with planes of scintillating bars. The combination of SciFi and the scintillating bars of the muon detector also act as a non-homogenous



hadronic calorimeter for the measurement of the energy of the hadronic jet produced in the neutrino interaction, and hence the neutrino energy. As the hadronic shower already starts developing in the target region, an average total length of the detector makes about  $11 \lambda_{\text{int}}$ , thus providing a good coverage of the hadronic showers.

The chemical treatment of the irradiated emulsions of the neutrino target are being performed in a dark room at CERN, equipped with the necessary tools to process 1200 emulsion films in one week. The entire thickness of the emulsion is analyzed using optical microscopes acquiring tomographic images at equally spaced depths. The total emulsion-film surface to be scanned in the first phase of the SND@LHC experiment requires at least five scanning systems fully devoted to this activity in order for the readout time to be approximately equal to the exposure time. The emulsion readout is being performed in dedicated laboratories at the Universities of Bologna and Naples (Italy), the University of Zurich (Switzerland), the Lebedev Physical Institute (Moscow, Russia) (Figure 5 [13]), and the CERN Emulsion Facility. The last one was completely equipped and prepared for operation in November 2021. The laboratories are equipped with automated optical microscopes, whereby the scanning speed of which, measured in terms of film surface per unit time, reaches  $\sim 180 \text{ cm}^2/\text{h}$ .

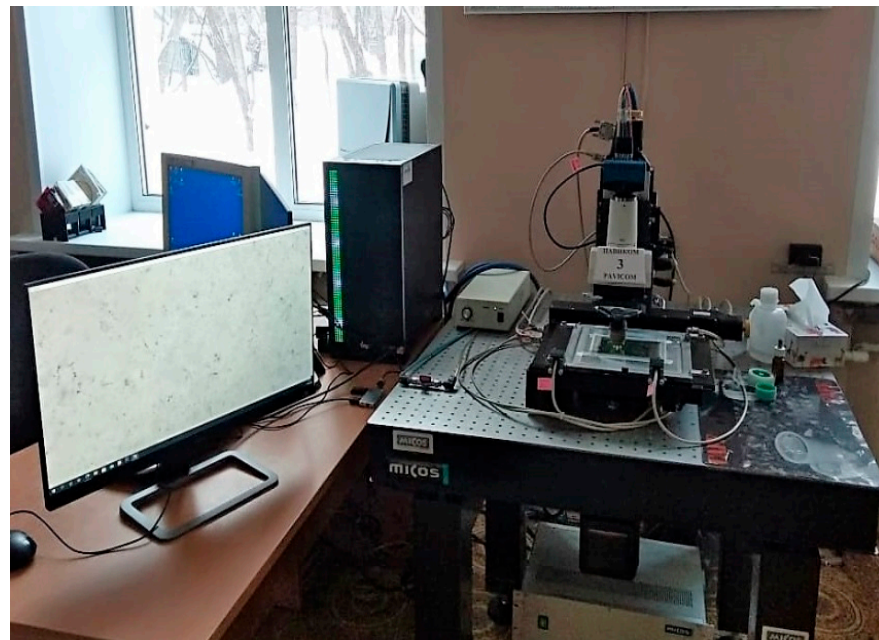


**Figure 5.** One of the scanning systems for the emulsion readout.

### 3. Reconstruction

Event reconstruction is performed in two stages, as shown in Figure 6. The first stage is the data-taking using the response of the electronic detectors. The second stage incorporates the emulsion data that are available about six months after the exposure. The occurrence of the neutrino interaction or FIP scattering is first detected by the target tracker and muon system (Figure 6a). Electromagnetic showers are absorbed within the target region and are therefore identified by the target tracker, while muons in the final state are reconstructed by the muon system. The determination of the neutrino flavor is made by identifying the charged lepton produced at the primary vertex (Figure 6b). Particularly, tau-leptons are identified through the observation of the tau decay vertex in the emulsion, along with the absence of any electron or muon in the primary vertex.

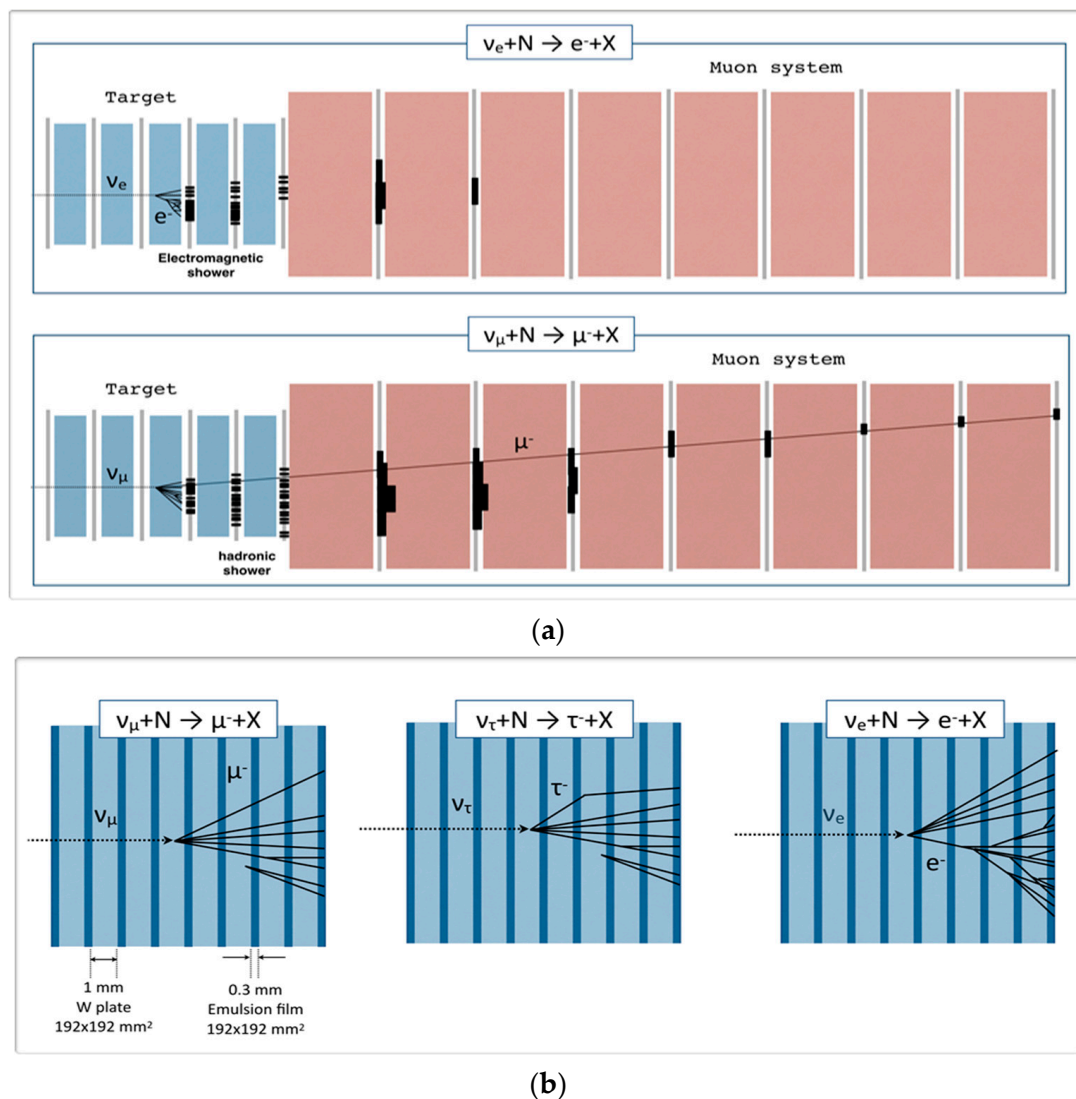


**Figure 6.** Event reconstruction: (a) the first stage (online, using electronic detectors); (b) the second stage (offline, using nuclear emulsions).

Two algorithms were developed for event identification. The first algorithm is based on the global topology of the event and does not depend on the efficiency of the track reconstruction. This algorithm is used to estimate the NC/CC ratio and provides a general veto for neutral current (NC) events. The second algorithm is based on muon track reconstruction and therefore can only be applied to events where such a track exists, that is mandatory for muon track coupling between electron detectors and emulsions. A significant parameter for the influence of the electron track with respect to the primary vertex allows for the identification of a  $\nu_e$  event. The  $\nu_\mu$  CC events can be distinguished using electronic detectors (the downstream stations of the muon system); the identification of  $\nu_e$  CC is quite challenging with electronic detectors since the pattern is similar to NC events. This is one of the topics addressed in the analysis. FIPs can be identified through their scattering-off atoms of the emulsion target material. In the case of FIPs elastic scattering-off atomic electrons, the experimental signature consists of an isolated recoil electron that can be identified through the development of an electromagnetic shower in the target region. For FIPs interacting elastically with a proton, instead, the isolated proton produces a hadronic shower in the detector.

#### 4. Data and First Results

On April 2022, one fifth of the target region was partially instrumented with emulsion films, together with a few independent small emulsion bricks to test the machine-induced background during the LHC commissioning, as the final step of the detector installation. A test with one brick with the first batch of emulsion films (Emulsion Run 0) was conducted in order to test the chemical compatibility of the tungsten plates with the emulsions, the light tightness of the wall box, and the uniformity of the track reconstruction within the brick. The track density in the emulsion films of the Emulsion Run 0 made 7000 tracks per  $\text{cm}^2$ .

The first results are presented in Figure 7, with the Gaussian fits leading to the widths  $\sigma_x \sim 9 \mu\text{m}$  for the position and  $\sigma_{Tx} \sim 8 \text{ mrad}$  for the slope as the tangent of the track angle in the  $zx$  plane. The presented Gaussian fits indicate a high accuracy of track reconstruction in the emulsion target.

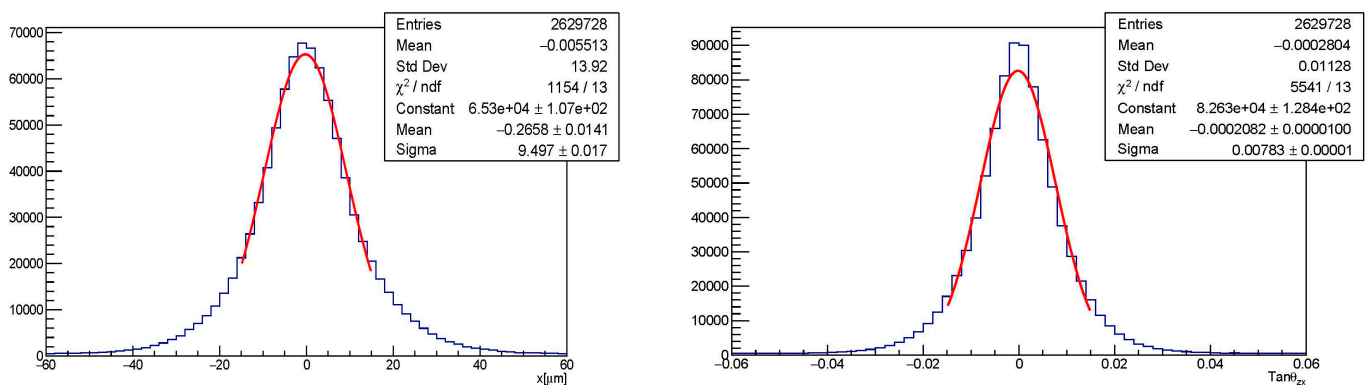


**Figure 7.** Distributions with the Gaussian fit (red) of the tracking resolution in  $x$  position (**left**) and in the slope as the tangent of the track angle in the  $zx$  plane,  $T_x = \text{Tan}(\theta_{zx})$  (**right**), for the Emulsion Run 0 data. “Std Dev” stays for the standard deviation, and “ndf” denotes the numbers of degrees of freedom in the Gaussian fit parameters shown.

According to estimates, emulsions can stand  $10^7$  tracks/ $\text{cm}^2$ . The track extrapolation between emulsions across a passive material layer becomes more complex when the track density is high; a level of  $10^5$  tracks/ $\text{cm}^2$  is regarded as a good condition. Thus, given the background estimates in T118 (Target line 18) LHC tunnel, one emulsion target exposure should not exceed  $30 \text{ fb}^{-1}$ . In view of the this luminosity that the LHC is expected to deliver during Run 3, it means that the emulsion target bricks should be replaced at least every two months of irradiation.

The first phase of the SND@LHC experiment was put into operation since the start of LHC Run 3 and was implemented during 2022. Emulsion Runs 1–3 were carried out using full emulsion targets with different luminosity exposures. The last one ended by the time of the LHC Run 2 technical shutdown on 28 November 2022 (see Figure 8).

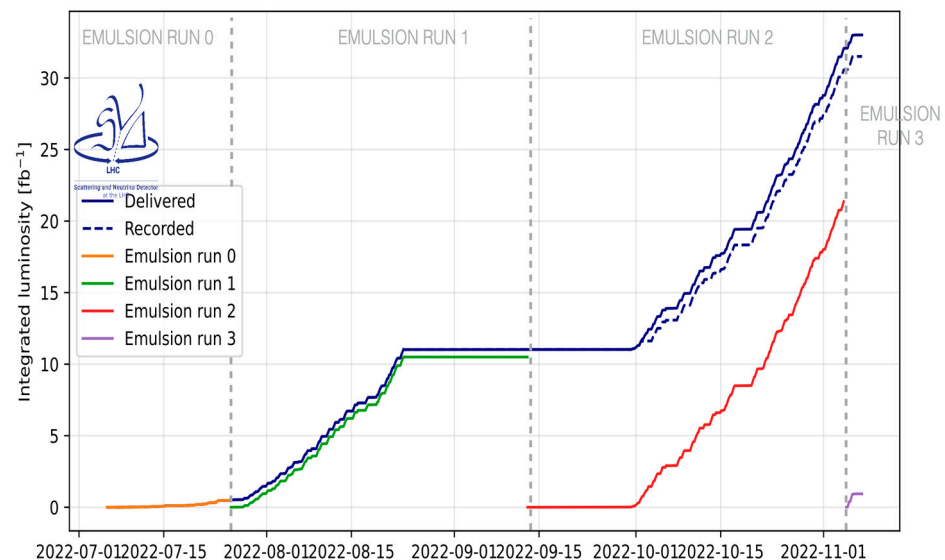


**Figure 8.** Status of the to-date SND@LHC exposures. In the “Delivered” sessions, the emulsion detector was exposed to the beam (with integrated luminosity of  $41.3 \text{ fb}^{-1}$ ). In the “Recorded” sessions, the emulsion detectors worked synchronously with the electronic ones ( $39.8 \text{ fb}^{-1}$ , or 96% of the “Delivered”).

## 5. Discussion

The SND@LHC experiment in its first phase accumulated the integrated luminosity of  $41.1 \text{ fb}^{-1}$ . The first stage of the data analysis is now in progress: the position and angular distributions of muon tracks are being reconstructed in the electronic detectors, and the search for neutrino candidate events is being performed.

The total surface to be scanned makes 3522 emulsion films with a total surface of  $130 \text{ m}^2$ , which requires at least six months of continuous operation of all microscopes. On the basis of reconstruction of the emulsion tracks, the background rejection, neutrino vertex identification, neutrino flavor identification, electromagnetic shower identification and energy measurements are planned to be performed. The emulsion data to be compared with the data from the electronic detectors. In the first phase of the experiment, one expects 217 CC and 68 NC neutrino interactions in the target.

**Author Contributions:** Conceptualization, N.P.; methodology, T.S.; validation, N.P., N.K. and T.S.; formal analysis, T.S.; investigation, N.K. and T.S.; resources, N.P.; data curation, T.S.; writing—original draft preparation, N.K.; writing—review and editing, N.P.; visualization, T.S.; supervision, N.P.; project administration, N.P.; funding acquisition, N.P. All authors have read and agreed to the published version of the manuscript.

**Funding:** This research received no external funding.

**Data Availability Statement:** The data are available upon reasonable request.

**Conflicts of Interest:** The authors declare no conflict of interest.

## References

1. Ahdida, C. et al. [SND@LHC Collaboration]. *SND@LHC—Scattering and Neutrino Detector at the LHC (Technical Proposal)*; Report CERN-LHCC-2021-003/LHCC-P-016; CERN: Geneva, Switzerland, 2021. Available online: <https://cds.cern.ch/record/2750060> (accessed on 25 March 2023).
2. Ahdida, C. et al. [The SHiP Collaboration]. *SND@LHC*. *arXiv* **2020**, arXiv:2002.08722. [[CrossRef](#)]
3. Acampora, G. et al. [The SND@LHC Collaboration]. *SND@LHC: The scattering and neutrino detector at the LHC*. *arXiv* **2022**, arXiv:2210.02784. [[CrossRef](#)]
4. Abreu, H. et al. [The FASER Collaboration]. Detecting and studying high-energy collider neutrinos with FASER at the LHC. *Eur. Phys. J. C* **2020**, *80*, 61. [[CrossRef](#)]



5. Lanfranchi, G.; Pospelov, M.; Schuster, P. The Search for Feebly-interacting particles. *Annu. Rev. Nucl. Part Sci.* **2020**, *71*, 279–313. [[CrossRef](#)]
6. Boyarsky, A.; Mikulenko, O.; Ovchinnikov, M.; Shchutska, L. Searches for new physics at SND@LHC. *J. High Energy Phys.* **2022**, *2022*, 6. [[CrossRef](#)]
7. Roesler, S.; Engel, R.; Ranft, J. The Monte Carlo event generator DPMJET-III. In *Advanced Monte Carlo for Radiation Physics, Particle Transport Simulation and Applications*; Kling, A., Barão, F.J.C., Nakagawa, M., Távora, L., Vaz, P., Eds.; Springer-Verlag: Berlin/Heidelberg, Germany, 2001. [[CrossRef](#)]
8. Böhlen, T.T.; Cerutti, F.; Chin, M.P.W.; Fasso, A.; Ferrari, A.; Ortega, P.G.; Mairani, A.; Sala, P.; Smirnov, G.; Vlachoudis, V. The FLUKA code: Developments and challenges for high energy and medical applications. *Nucl. Data Sheets* **2014**, *120*, 211–214. [[CrossRef](#)]
9. Ariga, A.; Ariga, T.; De Lellis, G.; Ereditato, A.; Niwa, K. Nuclear emulsions. In *Particle Physics Reference Library: Volume 2: Detectors for Particles and Radiation*; Fabjan, C.W., Schopper, H., Eds.; Springer Nature Switzerland AG: Cham, Switzerland, 2020; pp. 383–438. [[CrossRef](#)]
10. Agafonova, N. et al. [OPERA Collaboration]. Final results of the OPERA experiment on  $\nu\tau$  appearance in the CNGS beam. *Phys. Rev. Lett.* **2018**, *120*, 211801. [[CrossRef](#)] [[PubMed](#)]
11. Agafonova, N. et al. [The OPERA Collaboration]. Final results of the search for  $\nu\mu \rightarrow \nu e$  oscillations with the OPERA detector in the CNGS beam. *J. High Energy Phys.* **2018**, *2018*, 151. [[CrossRef](#)]
12. Agafonova, N.; Alexandrov, A.; Anokhina, A.; Aoki, S.; Ariga, A.; Ariga, T.; Bender, D.; Bertolin, A.; Bozza, C.; Brugnera, R.; et al. Procedure for short-lived particle detection in the OPERA experiment and its application to charm decays. *Eur. Phys. J. C* **2014**, *74*, 2986. [[CrossRef](#)]
13. Alexandrov, A.; Konovalova, N.; Okateva, N.; Polukhina, N.; Starkov, N.; Shchedrina, T. Upgrade and new applications of the automated high-tech scanning facility PAVICOM for data processing of track detectors. *Measurement* **2022**, *187*, 110244. [[CrossRef](#)]

**Disclaimer/Publisher's Note:** The statements, opinions and data contained in all publications are solely those of the individual author(s) and contributor(s) and not of MDPI and/or the editor(s). MDPI and/or the editor(s) disclaim responsibility for any injury to people or property resulting from any ideas, methods, instructions or products referred to in the content.